Bioresource Technology 169 (2014) 658–666

Contents lists available at ScienceDirect

Bioresource Technology

journal homepage: www.elsevier.com/locate/biortech

Pyrolysis kinetics of algal consortia grown using swine manure wastewater

Mahmoud A. Sharara, Nathan Holeman, Sammy S. Sadaka *, Thomas A. Costello

Biological and Agricultural Engineering Department, University of Arkansas – Division of Agriculture, AR, USA

HIGHLIGHTS

- Characterization of algae grown using swine manure slurry in different seasons.
- Determination of pyrolysis TG–DTG characteristics under different heating rates.
- Determination of apparent activation energies using isoconversional methods.
- Modeling algae consortia pyrolysis as four independent parallel reactions.

ARTICLE INFO

Article history:
Received 2 June 2014
Received in revised form 28 June 2014
Accepted 30 June 2014
Available online 16 July 2014

Keywords:
Microalgae
Phycoremediation
Pyrolysis
TGA
Kinetic modeling

ABSTRACT

In this study, pyrolysis kinetics of periphytic microalgae consortia grown using swine manure slurry in two seasonal climatic patterns in northwest Arkansas were investigated. Four heating rates (5, 10, 20 and 40 °C min^{-1}) were used to determine the pyrolysis kinetics. Differences in proximate, ultimate, and heating value analyses reflected variability in growing substrate conditions, i.e., flocculant use, manure slurry dilution, and differences in diurnal solar radiation and air temperature regimes. Peak decomposition temperature in algal harvests varied with changing the heating rate. Analyzing pyrolysis kinetics using differential and integral isoconversional methods (Friedman, Flynn–Wall–Ozawa, and Kissinger–Akahira–Sunose) showed strong dependency of apparent activation energy on the degree of conversion suggesting parallel reaction scheme. Consequently, the weight loss data in each thermogravimetric test was modeled using independent parallel reactions (IPR). The quality of fit (QOF) for the model ranged between 2.09% and 3.31% indicating a good agreement with the experimental data.

1. Introduction

Thermogravimetry is a powerful and versatile tool in understanding and modeling biomass reactions. It is also a quick and reliable approach to determine the moisture, organic matter, and ash contents in biomass (García et al., 2013). Other uses of thermogravimetric analysis (TGA) include quantification of the hemicellulose and α-cellulose contents in wood (Carrier et al., 2011), as well as evaluation of digestate stability during anaerobic digestion (Gómez et al., 2007). The predominant use of TGA, however, is to determine the rate of thermal decomposition for various feedstocks. A survey of the literature shows the importance of this analysis to the determination of decomposition kinetics of woody biomass (Gomez et al., 2005), crop residue (Mani et al., 2010), animal manures (Sharara and Sadaka, 2014), and municipal solid waste (Sanchez et al., 2009). However, the recent interest in aquatic biomass, as a biofuel and bioenergy crop, brought to light the dearth of thermogravimetric studies on this class of biomass.

Historically, microalgae mass-production was mostly accomplished to support aquaculture systems (Muller-Feuga, 2000) as well as to extract important bioactive compounds (Skulberg, 2004). Recently, however, interest in sustainable biofuel sources brought attention to microalgae due to the high lipid content in certain species, which can be converted via "transesterification" to biodiesel. The oil content in microalgae species such as *Schizochytrium* sp. can exceed 75% on a dry-weight basis (Demirbas and Fatih Demirbas, 2011). A vital ecological service that microalgae could provide is treatment of nutrient-rich wastewater effluents, i.e., phycoremediation. This particular service is becoming increasingly crucial with the increase in global urbanization, industrialization, and intensive cropping activities (Heathwaite, 2010).

Contamination of surface and ground water with nitrogen (N), phosphorous (P), polycyclic aromatic hydrocarbons (PAH), and

* Corresponding author. Tel.: +1 501 671 2298; fax: +1 501 671 2303.
E-mail address: ssadaka@uaex.edu (S.S. Sadaka).

http://dx.doi.org/10.1016/j.biortech.2014.06.111
0960-8524/

heavy metals is the primary cause behind hypoxic conditions, eutrophication, and the collapse of aquatic habitats in rivers and lakes (Conley et al., 2009). Uptake and biosorption of these contaminants by algal species has been investigated on a variety of wastewater substrates, i.e., municipal, industrial, and agricultural wastewater streams (Pittman et al., 2011). Adopting phycoremediation in livestock wastewater management can offer an added-advantage by minimizing phosphorus loss. Algal species were successfully grown on raw swine manure effluents, 9 g m^{-2} day^{-1}, but were found to be sensitive to the loading rates of N and P (Kebede-Westhead et al., 2006).

The harvested phycoremediation algae can be directed to a variety of uses such as composting, anaerobic digestion, and the extraction of lipids and sugars for biodiesel and ethanol production. Alternatively, the algal biomass can be utilized through thermochemical conversion processes. The end-use for a specific algae harvest is highly dependent on its composition. Algae used in water remediation are typically indigenous species grown in open systems that results in a diverse species consortium in the collected biomass. Thermogravimetric analyses can assist in the effort to characterize the harvested microalgae and to direct them to the optimal end-uses. For instance, TGA decomposition rate curves were proven effective in detecting and quantifying the lipid contents in *Chlorella* sp. (Na et al., 2011). Understanding the decomposition kinetics of microalgae in various atmospheres, in addition to providing insight into the proximate composition, is essential to the design and optimization of thermochemical conversion processes. There is a need in research for studies covering the thermal decomposition kinetics of mixed algae consortia grown for water remediation purposes, especially as part of sustainable livestock production scenarios. The goal of this research is to study the thermal decomposition of indigenous periphytic microalgae grown in an open water-remediation system for a swine production facility under nitrogen environment using thermogravimetric analysis (TGA).

2. Methods

2.1. Swine wastewater treatment system

Algal biomass was produced using open channel raceways lined with a growth medium for periphyton attachment and irrigated by circulation of swine-manure based wastewater. Algae consortia produced using two systems were investigated in this study. System 1 was a small system with 8 raceways that were each 15 cm wide by 3.0 m long. It was sited outdoors adjacent to the University of Arkansas Biological and Agricultural Engineering Research Lab, Fayetteville, Arkansas. System 2 was a larger pilot system with 4 raceways that were each 1.5 m wide by 61 m long. It was constructed at the University of Arkansas Swine Research Grower Facility, near Savoy Arkansas. The raceways in both systems were lined with specialty fibrous carpeting (proprietary fiber selection and layout intended to optimize periphyton growth, provided by Interface, Inc.) to maximize algae attachment during water circulation. System 1 was operated during the summer of 2013 (June–July) on swine manure slurries at different degrees of dilution to vary targeted starting ammonia (NH_3) concentrations between 5 and 40 mg L^{-1} (mg = 10^{-6} kg). Details of the NH_3 loading influence will be discussed in a separate publication. System 1 was seeded with mixed consortia which were collected from a local stream in Fayetteville, AR whereas System 2 was seeded from the mixed consortia harvested from System 1. Wastewater used in System 2 was pumped from swine slurry storage lagoon, then treated with alum (aluminum sulfate 14-hydrate granules, $Al_2(SO_4)_3{\cdot}14H_2O$, addition rate 2 g L^{-1}) to flocculate solids. After a 24 h settling period, the undiluted supernatant was removed for circulation in the raceway. System 2 was operated during the fall of 2013 (November–December). Both systems were open during production without any control over the growing algal species.

2.2. Algae collection and preparation methods

Harvest of algae was accomplished manually, in 5-day cycles, using a rubber-bladed squeegee for removal and collection of attached algae. Harvested algae were dried immediately or else stored at 4 °C for 24 h before drying. Subsamples of fresh algae were stored for analysis and species identification. One composite sample was collected from each algae consortium for the thermogravimetric analysis (TGA). Composite algae samples were dried at 105 °C for 24 h before grinding to 1 mm (Thomas Wiley® cutting mill-Model 3383L10, Swedesboro, NJ). A second grinding step, using a cutting mill (Polymix PX-MFC 90 D, Kinematica AG, Switzerland), was added to homogenize the dried samples and minimize mass transport resistance during thermogravimetric analysis. The algal solids used in the following tests and analyses all passed through a 200 μm sieve (μm = 10^{-6} m).

2.3. Proximate, ultimate, heating value and pH analyses

The remaining moisture was determined, in triplet samples, as the weight loss after drying at 105 °C, ASTM E871 – 82 (2006). Standard methods were also used to determine the volatile matter, ASTM E872 – 82 (2006), and ash content, ASTM D2974 – 87 (2007), while the fixed carbon (%) was determined by difference. Complete elemental analyses of representative samples from each algae harvest were performed in a specialized diagnostic laboratory (Huffman laboratories, Golden, CO, USA). The heating values were determined on sample triplets, according to standard ASTM D5865 – 12 (2012), using bomb calorimetry (Parr instruments, Model 1341, Moline, IL, USA). The pH of algal biomass was determined using a pH electrode (SB70P, SympHony, VWR, Radnor, PA, USA) after the dry, ground samples were diluted with deionized water, 10 mL per 1 g of sample, then vigorously stirred and allowed to stand for 1 h before measurement.

2.4. Thermogravimetric analysis methodology

A thermogravimetric analyzer (Model TGA 4000, PerkinElmer, Inc. Waltham, MA, USA) was used to study the decomposition behavior of the two algal harvests. Prior to the algae decomposition tests, a curie-point temperature calibration was performed using three reference materials, i.e., alumel, perkalloy, and Iron, according to the manufacturer's guidelines. Similarly, a weight calibration was performed, before tests, using the manufacturer supplied reference weight. Pyrolysis of each of two algae biomasses was studied under four different heating rates (5, 10, 20, and 40 °C min^{-1}) from 30 to 800 °C. Nitrogen gas was used to purge the sample (30 mL min^{-1}) to simulate pyrolysis conditions. The sample size was consistently kept at 5 ± 0.5 mg to minimize deviation (lag) between measured and actual sample temperatures, and to also ensure that the decomposition reactions were not transport-limited. For each sample, blank, clean crucibles were tested using the same thermal decomposition programs in order to adjust the weight baseline by compensating for the drag force acting on the crucible.

2.5. Decomposition kinetics

The decomposition is often expressed in terms of the conversion (α) which describes the change in sample weight, in a dimensionless form.

$$\alpha = \frac{W_o - W_t}{W_o - W_\infty} \quad (1)$$

W_o, W_t, and W_∞ are the sample weights at the beginning, at time t, and at the end of the decomposition stage, respectively. The rate of conversion ($d\alpha/dt$) is often expressed using an Arrhenius type expression.

$$\frac{d\alpha}{dt} = A \exp\left(\frac{-E_a}{RT}\right) f(\alpha) \quad (2)$$

A, E_a, R, and T are the pre-exponential coefficient (frequency factor), the activation energy, the universal gas constant, and the sample absolute temperature, respectively. $f(\alpha)$ represents the kinetic model that describes the rate of conversion dependence on the conversion, e.g., an n-order reaction model: $f(\alpha) = (1-\alpha)^n$.

Under a constant heating-rate ($\beta = dT/dt$), the time-dependence of the conversion rate can be transformed to a temperature-dependence which can be used to rewrite the differential form (Eq. (3)) or the integral form (Eq. (4)) of the decomposition kinetic expression.

$$\frac{d\alpha}{dT} = \frac{A}{\beta} \exp\left(\frac{-E_a}{RT}\right) f(\alpha) \quad (3)$$

$$g(\alpha) = \int_0^T \frac{A}{\beta} \exp\left(\frac{-E_a}{RT}\right) dT \quad (4)$$

The following sections will detail the different model-free (isoconversional) methods used to determine the apparent activation energies for algae pyrolysis.

2.5.1. Model-free (isoconversional) methods

Isoconversional methods overcome the requirement of determining the reaction model, $f(\alpha)$, in order to determine the activation energy, E_a. This is accomplished by simultaneously analyzing decomposition curves generated under different heating rates to extract the apparent kinetics data, i.e., E_a and $\ln A$, corresponding to each degree of conversion (α). Isoconversional methods are popular in biomass decomposition studies due to the fact that biomass, a natural biopolymer, undergoes a series of overlapping reactions, during pyrolysis or oxidation, which cannot be described accurately by one-step, global reaction model. The downside in isoconversional methods, however, is the inability to straightforwardly determine an exact model expression, $f(\alpha)$ or $g(\alpha)$, to describe the entire decomposition.

In this research, one differential isoconversional method, **Friedman method** (Friedman, 1965), and three integral isoconversional methods: **Kissinger's** (Blaine and Kissinger, 2012), **Flynn–Wall–Ozawa's** (Flynn and Wall, 1966; Ozawa, 1965), and **Kissinger–Akahira–Sunose's** (Starink, 2003) were used to determine the pyrolysis kinetics of the two algae harvests under study. Below is a brief description of each the methods.

2.5.1.1. Friedman method. Re-arranging Eq. (3), then linearizing it by taking the natural log of both sides of the equation

$$\ln\left(\beta \frac{d\alpha}{dT}\right) = \ln\left(A f(\alpha)\right) - \frac{E_a}{RT} \quad (5)$$

At each α, the above equation describes the linear relationship between $1/T$ and $\ln(\beta\, d\alpha/dT)$ with each point representing a tested heating rate. The slope of this line represents the activation energy term, E_a/RT, at this conversion degree whereas the intercept represents an expression combining the reaction model and the pre-exponential factor, $\ln(A f(\alpha))$. Calculating the slopes and intercepts at different α values, between 0.05 and 0.90, describe the kinetics of decomposition as a function of the conversion degree.

2.5.1.2. Kissinger method. This method determines the activation energy (E_a) and the pre-exponential factor (A) using the temperatures, T_{max} values, that correspond to peak decomposition rates, $(d\alpha/dt)_{max}$ in thermogravimetric tests under different heating rates (β). The temperature integral in Eq. (4) does not yield an analytical, closed-form solution. Therefore, it is alternatively presented as follows (Starink, 2003)

$$g(\alpha) = \frac{AE_a}{\beta R} p(x) \quad (6)$$

where $x = E_a/RT$, and the function $p(x)$ represents

$$p(x) = \int_x^\infty \frac{e^{-x}}{x^2} dx \quad (7)$$

Many approximations were derived to determine $p(x)$ numerically. In the Kissinger method, the Murray and White approximation (Starink, 2003), $p(x) \cong e^{-x}/x^2$, is used. The underlying assumption in this method is that the decomposition follows a first-order reaction model, i.e., $f(\alpha) = (1-\alpha)$. Eq. (8) details the relationship between T_{max}, β, and E_a and A.

$$\ln\left(\frac{\beta}{T_{max}^2}\right) = \ln\left(\frac{AR}{E_a}\right) - \frac{E_a}{RT_{max}} \quad (8)$$

By plotting $\ln \beta/T_{max}^2$ against $(1/T_{max})$, the activation energy (E_a/R) and the pre-exponential factor, $\ln(AR/E_a)$, terms can be determined, respectively, as the slope and the intercept of the resulting straight-line.

2.5.1.3. Kissinger–Akahira–Sunose (KAS) method. A modified form of Kissinger's method that was described earlier, KAS method dispenses with the kinetic model assumption, and the use of only the peak decomposition data. Instead, KAS is an integral method that relies on the different (α) values instead of the single value corresponding to peak decomposition ($d\alpha/dt$).

Eq. (8) can then be rearranged and linearized

$$\ln\left(\frac{\beta}{T^2}\right) = \ln\left[\frac{AR}{E_a}\right] - \ln\left(g(\alpha)\right) - \frac{E_a}{RT} \quad (9)$$

The slope of the straight lines formed by plotting $\ln(\beta/T^2)$ against $1/T$ at each degree of conversion (α), with the points corresponding to the different β values, yields the activation energy, E_a, corresponding to that conversion degree.

2.5.1.4. Flynn–Wall–Ozawa (FWO) method. In this method, the Doyle's approximation (Doyle, 1962) to the temperature integral, $p(x)$, is applied: $p(x) \cong -5.33 - 1.05x$. The linearized form of Eq. (4) becomes:

$$\ln \beta = \ln\left[\frac{AE_a}{Rg(\alpha)}\right] - 5.33 - 1.052\left(\frac{E_a}{RT}\right) \quad (10)$$

At each degree of conversion (α), $\ln \beta$ and $1/T$ corresponding to each heating rate are fitted into a straight line. The slope, $(-1.052E_a/R)$, represents the apparent activation energy term, while the intercept is a coupled expression of the reaction model in the integral form, $g(\alpha)$, the apparent activation energy E_a, and the frequency factor, A.

2.5.2. Kinetic modeling of algae pyrolysis

In order to investigate the pyrolysis of the two algae consortia, the weight loss was modeled as a series of overlapping independent, parallel reactions taking place between 100 and 700 °C. This approach was presented elsewhere as a deconvolution step necessary to understand the devolatilization of a biopolymer by modeling the various pseudo-components contributing to its overall decomposition. In this study, algae pyrolysis was modeled as 4

independent, 1st order reactions. The rate of conversion ($d\alpha/dt$) for pseudo-component (N) is:

$$\frac{d\alpha_N}{dt} = A_N \exp\left(\frac{-E_{a\,N}}{RT}\right)(1-\alpha_N), \quad \text{where } N = 1\ldots4 \tag{11}$$

Consequently, the total rate of conversion ($d\alpha_{\text{Total}}/dt$) can be determined from the individual pseudo-components using the following expression:

$$\frac{d\alpha_{\text{Total}}}{dt} = \sum_{i=1}^{N} w_i \frac{d\alpha_N}{dt}, \quad \text{and} \sum_{i=1}^{N} w_i = 1 \tag{12}$$

The quantity, w_i, represents the contribution of each individual pseudo-component to the overall sample conversion. The conversion rate can be converted to the mass loss rate using the following relation:

$$\frac{dm_{\text{calc}}}{dt} = -(m_o - m_f)\frac{d\alpha_{\text{Total}}}{dt} \tag{13}$$

m_o and m_f represent the initial and final sample weights. Numerical integration between the temperatures of interest, i.e., 100–700 °C in this study, yields the computed overall weight, m_{calc}. The parameters of each reaction, i.e., A, E_a, and w were determined by nonlinear minimization of an objective function (O.F.) which represents the sum of squared differences between observed sample mass loss rate, dm_{obs}/dt, and the calculated mass loss rate, dm_{calc}/dt:

$$\text{O.F.} = \sum_{i=1}^{N_p}\left(\frac{dm_{\text{calc}}}{dt} - \frac{dm_{\text{obs}}}{dt}\right)^2 \tag{14}$$

In this study, the total number of points, N_p, used in reaction modeling for each thermogram was 300 points. The quality of fit, QOF (%), for the weight loss derivative (DTG) and the weight loss (TG) were determined using the following expressions:

$$\text{QOF}_{\text{DTG}}(\%) = 100\left(\frac{\sqrt{\sum_{i=1}^{N_p}\left(\frac{dm_{\text{calc}}}{dt} - \frac{dm_{\text{obs}}}{dt}\right)^2}}{N_p}\right) \Big/ \left|\frac{dm_{\text{obs}}}{dt}\right|_{\max} \tag{15}$$

$$\text{QOF}_{\text{TG}}(\%) = 100\left(\frac{\sqrt{\sum_{i=1}^{N_p}(m_{\text{calc}} - m_{\text{obs}})^2}}{N_p}\right) \Big/ (m_{\text{obs}})_{\max} \tag{16}$$

Numerical integration was performed using a numerical integrator for stiff-equations, (**ODE15s)** while the constrained nonlinear minimization was performed using the (**fmincon**) function, both of which are part of the MATLAB software package (MATLAB R2013b, The Mathworks, Inc., Natick, MA, USA).

3. Results and discussions

3.1. Species identification

The harvested microalgae species were inspected non-quantitatively using optical microscopy. The microalgae consortium in each harvest, i.e., Algae 1 and Algae 2, consisted mostly of filamentous microalgae mixtures in addition to diatoms. The most common filamentous genus identified in Algae 1 was *Mougeotia*, while the genus *Cladophora* dominated Algae 2 harvest. Both genera are common fresh-water microalgae, which were reported to be tolerant of a wide range of growing conditions (Higgins et al., 2008; Morris, 1982). In a study of algal growths in Lake Mead (Nevada-Arizona, USA), Morris (1982) also reported the predominance of *Mougeotia* species, in certain monitoring stations during the summer months (June–July) which then changed to *Cladophora* and *Stigeoclonium* during the months of October and November.

3.2. Proximate analysis

Table 1 shows the results of proximate analysis of the two algae. The low moisture content in both harvests, around 5% wet-basis, represents the moisture absorbed after drying and during sample preparation. Comparison of proximate analysis results for the two algae harvests showed significant differences (t-test, $p < 0.01$) in volatile matter, fixed carbon, and ash contents. The ash contents observed in both algae consortia: 20% in Algae 1 and 32% in Algae 2 are noticeably high in comparison to the ash contents of terrestrial biomass (wood, grasses, and crop residue) which are below 10 wt.%. This is explained by algae's high potential for mineral biosorption and due to their simple cellular structures. The ash content in aquatic biomass vary drastically from less than 10% (Gai et al., 2013) to more than 50% (Zhao et al., 2013), according to type of alga and growth conditions. Algae grown on wastewater or high-mineral effluents in open ponds/raceways are expected to contain higher ash than algae produced in a closed-system on low-minerals water. The difference in ash contents, 12 percentage points, in this study could be attributed to use of the alum flocculant, $Al_2(SO_4)_3{\cdot}14H_2O$, on the swine manure slurries used to grow Algae 2. The high percentages of Al_2O_3 and SO_3 found in Algae 2 ash residue, 19.86% and 10.25%, compared to Algae 1, 1.93% and 4.54%, respectively, supports this hypothesis (Table 1). This difference in the ash contents also explains the relatively low volatile matter and fixed carbon contents observed in Algae 2 when compared to Algae 1.

3.3. Elemental composition, and higher heating value

Percentages of the main organic elements: carbon (C), hydrogen (H), nitrogen (N), and oxygen (O), in both algae are shown in Table 1. Algae 1 sample showed higher content of organic elements when compared to Algae 2 sample, except for N. These differences

Table 1
Proximate, ultimate, ash, calorific value, and pH analyses for the two algae consortia studied.

	Algae 1	Algae 2
Proximate analysis (wt.%*)		
Moisture	5.14	5.09
Volatile matter	64.49	56.30
Fixed carbon**	10.41	6.32
Ash	19.96	32.29
Ultimate analysis (wt.%)		
C	41.51	33.79
H	5.59	4.73
N	5.40	6.35
S	0.51	1.57
O**	27.03	21.27
Ash	19.96	32.29
Ash analysis (wt.%)		
Al_2O_3	1.93	19.86
SiO_2	14.57	16.44
P_2O_5	15.69	15.27
K_2O	6.57	12.09
SO_3	4.54	10.25
CaO	37.15	9.85
Na_2O	3.08	4.88
MgO	4.46	4.06
Fe_2O_3	1.42	3.50
MnO	0.08	0.17
TiO_2	0.06	0.15
HHV*** ($kJ\ g^{-1}$)	16.63	14.53
pH	6.88	7.69

* Weight-basis percentage.
** By difference.
*** Higher heating value.

are attributable, as discussed earlier, to the use of metal salt to precipitate the suspended solids in the manure slurry used in Algae 2 production. By contrast, the higher N content in Algae 2 is due to the elimination of slurry dilution, which was employed in growing the Algae 1 consortia. N loading was reported to influence the lipid and protein in the algal biomass (Xin et al., 2010). In lipid production from microalgae, a nutrient stress is typically imposed by reducing N-loading to induce lipid production and storage in algae cells. In phycoremediation, by contrast, algae are grown on N-rich substrates, which increase the protein content in the cells. From their N contents, the protein content in Algae 1 and 2 can be estimated using Jones' factor of 6.25 (Jones, 1941) to be 33.8% and 39.7%, respectively. Unlike terrestrial biomasses, which consist primarily of cellulose, hemicellulose, and lignin, microalgae are single cell organisms that consist of carbohydrates, proteins, and lipids. This structural difference can be observed in the stoichiometric expressions for Algae 1: $CH_{1.62}N_{0.11}O_{0.49}$ and Algae 2: $CH_{1.68}N_{0.16}O_{0.47}$, as compared to that for hybrid poplar wood (Jenkins et al., 1998): $CH_{1.45}N_{0.01}O_{0.60}$.

The difference observed in the higher heating values (HHV) between the studied algae harvests, 16.6 kJ g^{-1} in Algae 1, and 14.5 kJ g^{-1} in Algae 2, could be attributed to the difference in the ash contents. Calculating the dry, ash-free HHV (DAF), using the ash contents and the dry-basis HHVs in Table 1, shows both algae to have similar energy contents, i.e., 21 kJ g_{DAF}^{-1}.

3.4. Thermogravimetric analysis

With the temperature increase, the samples underwent a series of endothermic and exothermic reactions, which involved varying degrees of weight-loss (devolatilization) and structural change to the sample matrix. In both algae consortia, decomposition temperatures increased with increasing the heating rate (β). Doubling β led to an increase between 7 and 9 °C for the entire weight loss curve. Similarly, the rate of weight loss was observed to double with each doubling of the heating rate. In Algae 1, the pyrolysis resulted in a weight loss of 69–72% of initial weight whereas in Algae 2 the weight loss ranged between 62% and 67% over the entire temperature range, 30–800 °C. The difference in ash contents between the two algal consortia was reflected in difference between overall weight-loss.

During algae pyrolysis, the weight loss can be divided into three consecutive stages: ***drying***, ***active pyrolysis***, and ***passive pyrolysis***. Drying, which typically takes place below 110 °C, is the first step in algae pyrolysis and it involves the evaporation of both free and hygroscopic water in the sample matrix. In this step the initial weight dropped around 5% with the corresponding DTG peak at around 100 °C. After drying, the samples underwent a brief induction period, between 110 and 150 °C, in which the weight loss was minimal.

In pyrolysis, most of the weight loss takes place, between 150 and 550 °C, during the active pyrolysis stage. This weight loss represents the thermal depolymerization and volatilization of various organic matter (volatile matter) components. Algae 1 lost 58% of total weight during the active pyrolysis step compared to only 50% weight-loss in Algae 2. Despite the similarity in peak decomposition temperatures in the two consortia (Table 2), the maximum decomposition rates for Algae 1 samples, 0.44–0.48% $°C^{-1}$, were consistently higher than those observed for Algae 2, 0.33–0.37% $°C^{-1}$.

In biopolymers such as microalgae, the thermal decomposition represents the summation of decomposition profiles for the individual components. Given the wide variability between microalgae species, in terms of main ingredients' concentration and composition, the decomposition profiles under pyrolysis can vary greatly. Maddi et al. (2011) compared pyrolysis thermograms of *Lyngbya* sp. and *Cladophora* sp., and attributed the dissimilarity to differences in protein compositions (Maddi et al., 2011). In this study, the seasonal variability between consortia induced differences in algal community compositions, which were reflected in the respective decomposition profiles. In both consortia, however, the main decomposition peak took place in the range associated with carbohydrates and proteins indicating a similarity in the main composition. Furthermore, the peak associated with lipids decomposition (above 390 °C) (Na et al., 2011) was only a small shoulder in both consortia, indicating low lipid contents.

During passive-pyrolysis ($T > 550$ °C), both algae harvests showed minimal weight-loss, which is characteristic of char pyrolysis. A minor decomposition peak (0.06 % °C) which was observed in Algae 1 between 650 and 700 °C was not observed in Algae 2. In studying the pyrolysis of *Chlorella vulgaris*, Agrawal and Chakraborty (2013) attributed a similar high temperature weight-loss peak (at 700 °C) to a char gasification step, which was explained as CO_2 loss (Agrawal and Chakraborty, 2013). Maddi et al. (2011) also reported a high temperature peak during the decomposition of *Cladophora sp.* but could not identify the component associated with it. The kinetics of decomposition for both algae consortia during the active pyrolysis stage, 150–550 °C, will be discussed in the following section.

3.5. Pyrolysis kinetics

The temperature-conversion data in each algae sample (Fig. 1) was used to determine the decomposition kinetics during the active pyrolysis stage (150–550 °C). The conversion profile for each algae consortium approximates a sigmoidal function, which is typically associated with the autocatalytic reactions involved in pyrolysis (McCoy, 1999).

The kinetics determined using isoconversional methods, i.e., activation energy and pre-exponential term, are detailed in Table 3. Both isoconversional and integral methods showed strong correlation coefficients (r) and high significance (p-value < 0.01). In each algae consortium, the KAS and FWO activation energy values were very close, within 2%, at each conversion degree. Activation energies determined using Friedman method, on the other hand, were consistently higher than KAS and FWO, at times by 12%, as shown in Fig. 2. This difference in the activation energies, between the differential and integral methods, could be attributed to the numerical differentiation step necessary to determine the kinetics in Friedman method. Although Friedman method does not rely on

Table 2
Pyrolysis temperature (°C) and weight loss (%) corresponding to peak decomposition rate (% $°C^{-1}$) in both algae consortia.

Heating rate (°C min^{-1})	Algae 1			Algae 2		
	$-(dW/dT)_p$ (% $°C^{-1}$)	T_p (°C)	WL_p (%)	$-(dW/dT)_p$ (% $°C^{-1}$)	T_p (°C)	WL_p (%)
5	0.48	298.58	28.4	0.36	302.16	24.4
10	0.47	308.01	28.2	0.37	309.30	23.9
20	0.44	315.72	27.3	0.33	317.28	23.9
40	0.45	328.31	27.6	0.33	328.64	24.3

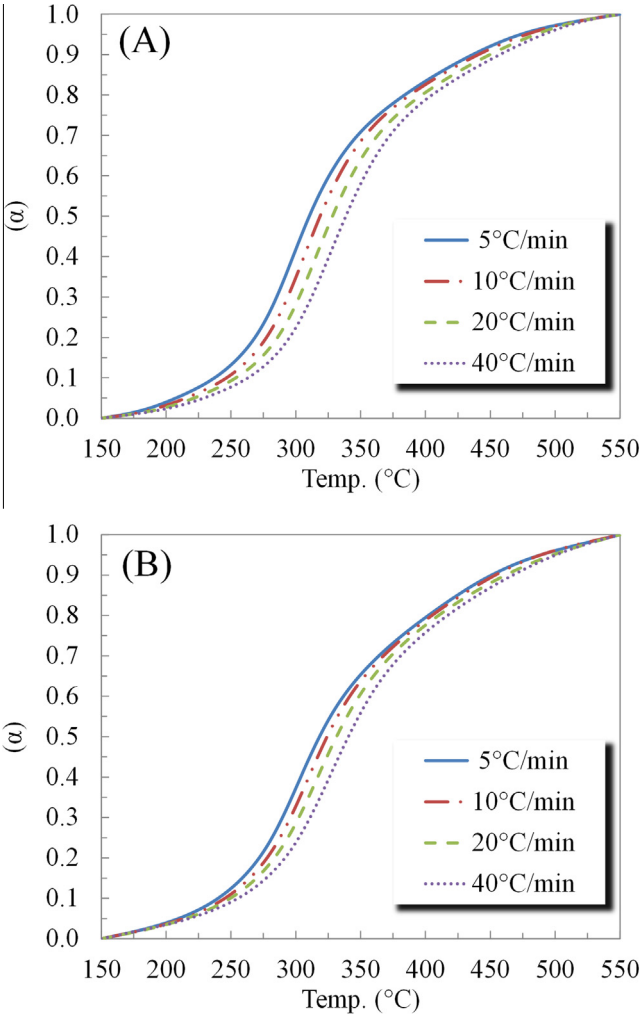

Fig. 1. Conversion-temperature (α–T) curves for (A) algae 1, and (B) algae 2 under different heating rates: β = 5, 10, 20, and 40 °C min^{-1}.

the integral approximation which is crucial to the integral methods, the numerical differentiation used in this method magnifies the instrument noise which necessitates data smoothing prior to analysis thus introducing a degree of uncertainty. The activation energies calculated using Kissinger method were 213.4 and 247.8 kJ mol^{-1} for Algae 1 and Algae 2, respectively. These values were constant over the entire range of conversion since they represent one data point, α–T pair, from each thermogram. By contrast, the activation energies computed using Friedman, KAS and FWO methods showed a strong dependence on the degree of conversion (α) in each algae consortium. This dependence, however, can be divided into three stages: $\alpha < 0.20$ where the activation energies fluctuated strongly with the conversion, $0.20 \leqslant \alpha \leqslant 0.60$ where the activation energies were not strongly dependent on the conversion degree, and finally, $0.60 < \alpha$ where the activation energies increased dramatically with the progress of decomposition. The increased $E_a - \alpha$ dependence in polymers was associated with parallel reactions, each having different activation energy (Vyazovkin, 1996). Yao et al. (2008) suggested that multistep decomposition mechanisms are the cause for increases E_a at $\alpha > 0.7$ during the pyrolysis of natural fibers (Yao et al., 2008). It is worth noting, however, that the activation energy estimated using Kissinger method closely represents the mean activation energy value using Friedman, KAS and FWO during constant activation energy zone, i.e., $0.20 \leqslant \alpha \leqslant 0.60$.

Results of pyrolysis modeling using independent parallel reactions (IPR) are detailed in Table 4 as well as in Figs. 3 and 4. The IPR model closely captured the weight loss profiles observed during active and passive pyrolysis stages for both algae harvests as shown in Fig. 3. The quality of fit (QOF_{DTG} %) ranged between 2.09% and 3.31% indicating only minor deviations between calculated and observed weight loss data. First-order reaction model appears to be capable of describing microalgae pyrolysis reactions satisfactorily. Earlier studies used this model to describe the pyrolysis kinetics of various biomass residues such as cardoon stems and leaves, and rice hulls (Teng and Wei, 1998; Damartzis et al., 2011). The apparent activation energies for Algae 1 pyrolysis reactions ranged from 33.26 to 97.66 kJ mol^{-1} while the apparent activation energies for Algae 2 pyrolysis reactions varied between 33.87 and 97.36 kJ mol^{-1}. Contribution of the modeled pseudo-components to the overall decomposition rate is detailed in Fig. 4. In both consortia, the peak devolatilization of each pseudo-component took place at a different temperature, starting at 100–120 °C for pseudo-component 1(47.00–49.65 kJ mol^{-1}) which represents the devolatilization of moisture and light hydrocarbons. Between 300 and 400 °C, both pseudo-components 2 and 3 showed overlapping peak devolatilization representing

Table 3
The pyrolysis activation energy (E_a), and intercept term (ln z) corresponding to different degrees of conversion (α) for Algae 1 and Algae 2 using Friedman, Kissinger–Akahira–Sunose (KAS), Flynn–Wall–Ozawa (FWO), and Kissinger methods.

	(α)	Friedman method			KAS method			FWO method		
		E_a (kJ mol^{-1})	ln z (s^{-1})	r	E_a (kJ mol^{-1})	ln z (s^{-1})	r	E_a (kJ mol^{-1})	ln z (s^{-1})	r
Algae 1	0.2	203.3	37.319	1.000	195.7	32.461	1.000	194.7	47.098	1.000
	0.3	210.1	37.856	0.999	205.1	33.158	1.000	204.0	47.855	1.000
	0.4	213.7	37.738	0.999	208.6	32.874	1.000	207.5	47.617	1.000
	0.5	223.4	38.709	0.999	213.9	32.984	1.000	212.8	47.770	1.000
	0.6	247.8	42.195	0.998	228.8	34.835	0.999	227.2	49.670	0.999
	0.7	296.0	49.348	0.995	267.0	40.565	0.996	263.8	55.467	0.996
	0.8	361.7	57.759	0.991	343.9	51.735	0.990	337.5	66.742	0.990
Kissinger method		213.4	39.815*	0.998						
Algae 2	0.2	263.1	50.229	0.997	267.2	48.025	0.997	262.7	62.662	0.998
	0.3	265.3	49.248	0.997	264.9	45.597	0.998	260.9	60.300	0.998
	0.4	271.6	49.269	0.997	266.8	44.580	0.997	262.9	59.334	0.997
	0.5	290.4	51.609	0.996	276.7	45.197	0.996	272.6	60.000	0.997
	0.6	345.6	60.407	0.994	313.8	50.767	0.994	308.1	65.628	0.995
	0.7	454.5	77.656	0.991	417.3	67.603	0.990	406.9	82.544	0.990
	0.8	538.3	87.512	0.984	527.9	82.781	0.984	512.6	97.834	0.985
Kissinger method		247.8	46.886*	0.999						

* ln A (s^{-1}).

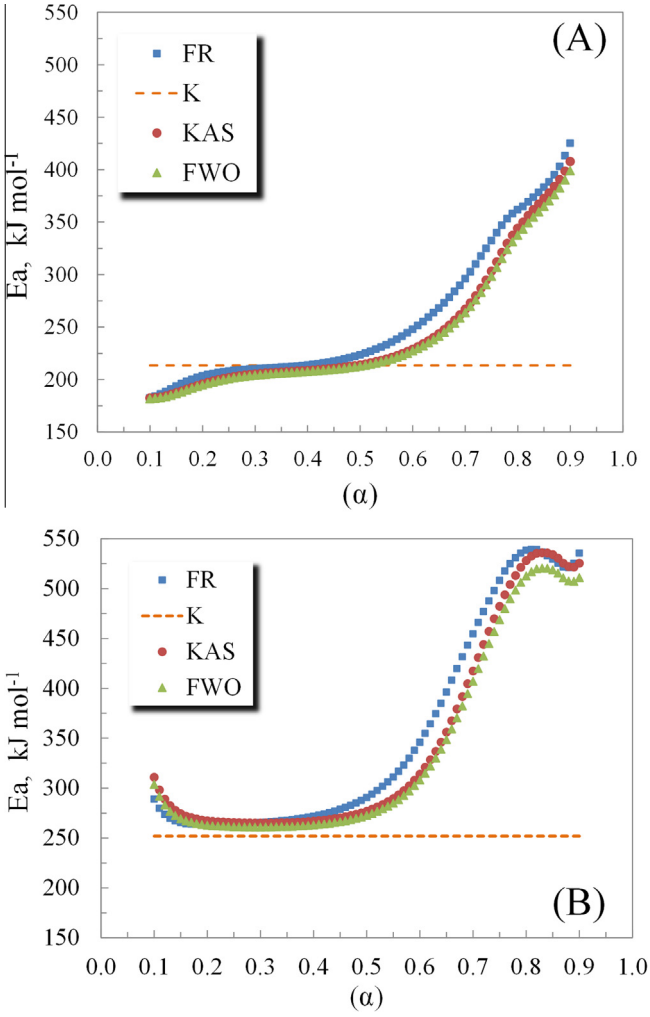

Fig. 2. The activation energy (E_a, kJ mol^{-1}) corresponding to the different degrees of conversion (α) during pyrolysis of: (A) Algae 1, and (B) Algae 2 using the following methods: Friedman (FR), Kissinger (K), Kissinger–Akahira–Sunose (KAS), and Flynn–Wall–Ozawa (FWO).

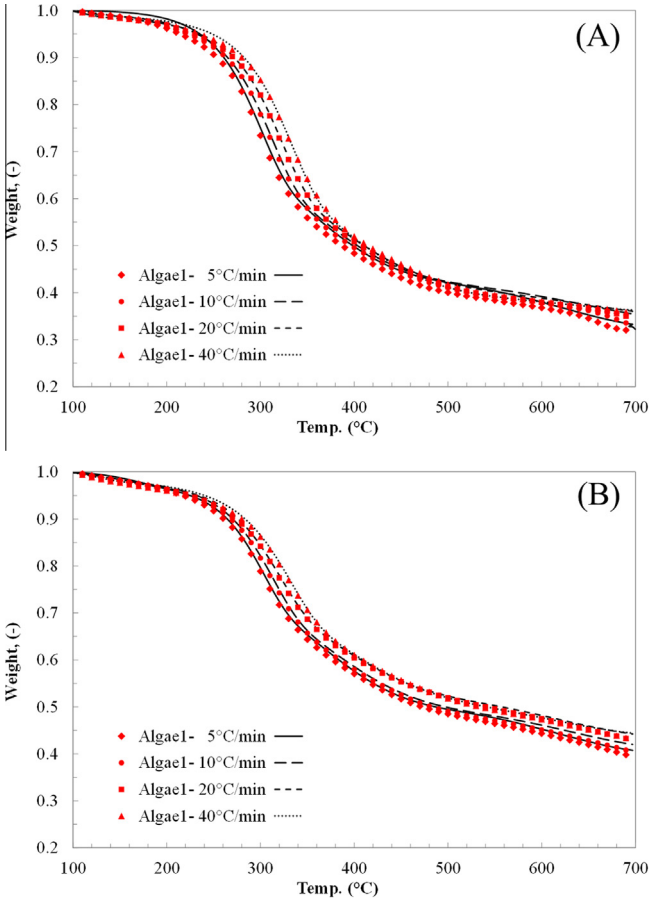

Fig. 3. Comparison between observed weight loss (markers) and calculated weight loss (lines) using independent parallel reactions (IPR) model for Algae 1 (A) and Algae 2 (B).

the bulk of the total weight loss (between 72% and 92% of total weight loss) (Table 4). Decomposition peak for reaction 2, as shown in Fig. 4, coincided with the overall peak decomposition observed in both algae as listed in Table 2. The two overlapping peaks: reactions 2 and 3 in both consortia appear to represent the decomposition of the main algae ingredients, *i.e.*, protein and starch. The decomposition peaks of individual starch and protein model substances: corn starch and Lysozyme protein (Maddi et al., 2011) appear to resemble the overlapped peaks in Fig. 4. The fourth pseudo-component showed peak decomposition around 600 °C, which represents the passive pyrolysis weight loss.

The differences observed between the apparent activation energies determined using isoconversional methods, and those

Table 4
Pyrolysis kinetics of the two algae consortia as modeled using Independent parallel reactions (IPR) model.

Reaction	Kinetics	Algae 1				Algae 2			
		5 °C min^{-1}	10 °C min^{-1}	20 °C min^{-1}	40 °C min^{-1}	5 °C min^{-1}	10 °C min^{-1}	20 °C min^{-1}	40 °C min^{-1}
1	w_1	0.11	0.01	0.02	0.02	0.04	0.03	0.05	0.03
	A_1 (s^{-1})	3.3E+01	3.8E+04	8.6E+04	5.4E+04	1.0E+03	4.3E+03	1.0E+02	9.0E+04
	E_{a1} (kJ mol^{-1})	47.00	49.17	49.65	48.57	47.06	46.20	32.89	49.63
2	w_2	0.31	0.36	0.39	0.42	0.29	0.30	0.35	0.31
	A_2 (s^{-1})	2.1E+06	3.1E+06	3.6E+06	5.3E+06	2.1E+06	2.3E+06	2.7E+05	4.1E+06
	E_{a2} (kJ mol^{-1})	97.09	97.66	97.03	97.24	97.36	96.35	84.23	95.86
3	w_3	0.41	0.49	0.49	0.50	0.49	0.52	0.43	0.51
	A_3 (s^{-1})	1.8E+00	1.1E+00	1.7E+00	4.9E+00	1.8E+00	1.2E+00	5.5E+00	3.6E+00
	E_{a3} (kJ mol^{-1})	39.59	33.60	33.26	35.77	39.59	34.42	39.42	33.87
4	w_4	0.16	0.14	0.11	0.07	0.18	0.15	0.17	0.15
	A_4 (s^{-1})	3.5E+01	1.4E+01	2.8E+01	8.1E+01	3.8E+01	8.6E+01	8.5E+01	8.1E+01
	E_{a4} (kJ mol^{-1})	78.06	69.37	69.35	69.28	78.03	80.49	74.27	69.10
QOF*	DTG (%)	3.31	2.89	2.80	2.76	2.78	2.09	2.54	3.03
	TG (%)	1.62	1.03	0.61	0.55	0.80	0.75	0.56	0.53

* Quality of fit.

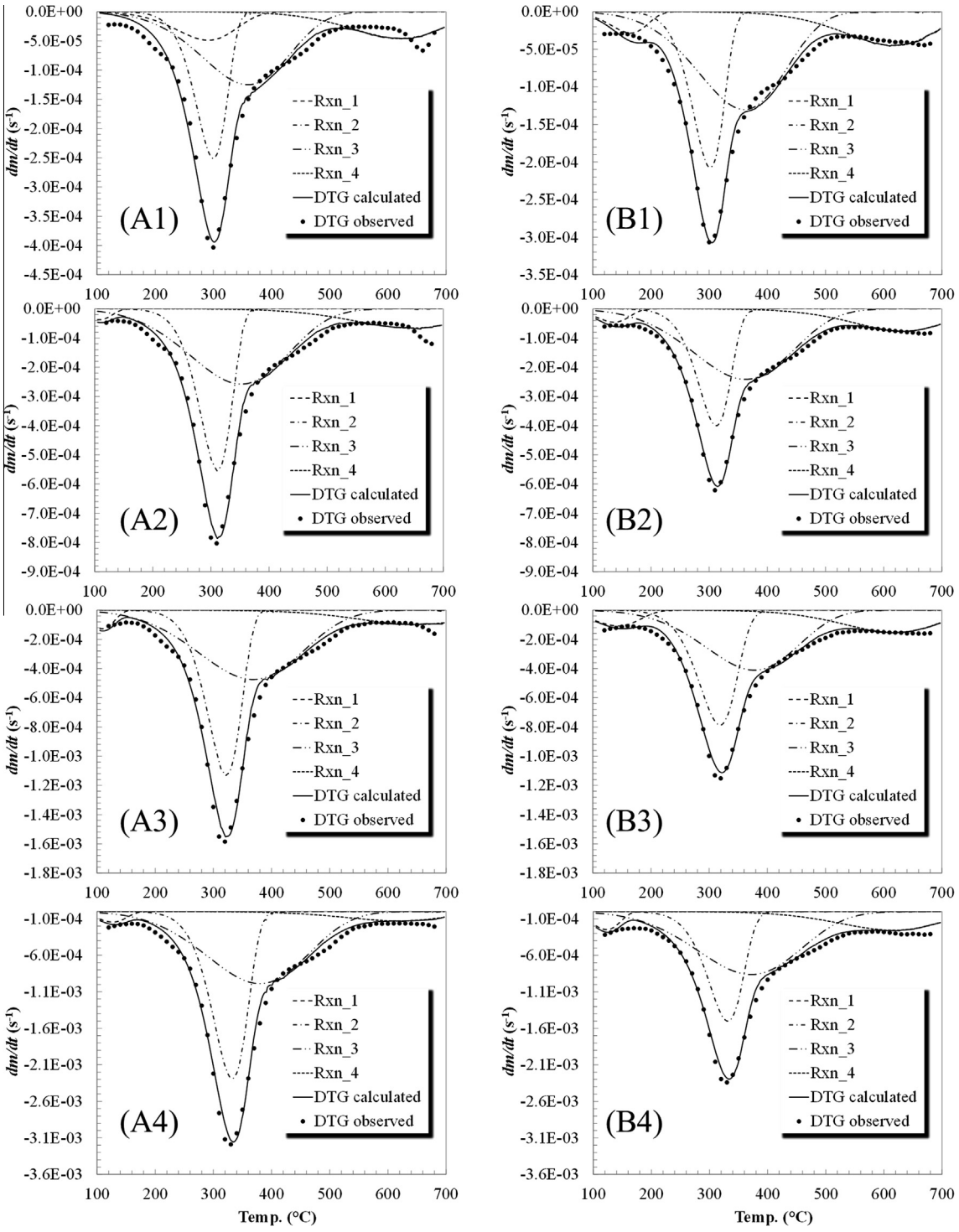

Fig. 4. Comparison between observed weight loss (markers) and calculated weight loss (lines) using independent parallel reactions (IPR) model for Algae 1 (A) and Algae 2 (B) with the different heating rates, 5, 10, 20 and 40 °C min^{-1}, represented by the numerals 1, 2, 3 and 4, respectively.

determined using the independent parallel reactions (IPR) model are attributed in part to the reaction model used. While isoconversional methods determine an overall apparent activation energy without specifying a reaction model (model-free), modeling the pyrolysis kinetics necessitate the assumption of a reaction model with multiple activation energies for the different reactions involved. Damartzis et al. (2011) showed a similar contrast between the activation energies of cardoon pyrolysis determined using isoconversional methods and those using IPR model (Damartzis et al., 2011). They suggested that isoconversional methods are most suited to qualitative evaluations of the pyrolysis process, whereas models such as IPR are more suitable quantitatively to study and model the pyrolysis process.

It is worth noting, however, that in terrestrial biomasses such as wood, and crop residues, the individual pseudo-components resulting from kinetic modeling, such as IPR, can be easily associated with original biomass ingredients, *i.e.*, cellulose, hemicellulose and lignin. However, given the species heterogeneity of the algal

consortia investigated here, not to mention the complex structures in individual algal species, it is not possible to map the modeled pseudo-component to specific structural components or intermediate species. Nonetheless, coupling these pseudo-components to the evolved species, via spectral analysis, can offer better understanding of the original species undergoing decomposition.

4. Conclusions

- The algae genus *Mougeotia* was the common genus in the Algae 1 harvest, while the genus *Cladophora* was predominant in the Algae 2 harvest.
- In isoconversional methods, the apparent activation energies for pyrolysis of Algae 1 were lower than Algae 2 pyrolysis.
- Friedman method activation energy values were within 12% of Kissinger–Akahira–Sunose (KAS) and Flynn–Wall–Ozawa (FWO) values.
- The activation energy dependence on conversion suggests complex reaction schemes which should not be reduced to a single-step reaction.
- The pyrolysis kinetics of each consortium was modeled using independent parallel reaction (IPR) model as a group of four parallel, independent, first-order reactions.

Acknowledgements

This research is part of the program "Climate Change Mitigation and Adaptation in Agriculture," and is supported by Agriculture and Food Research Initiative Competitive Grant no. 2011-68002-30208 from the USDA National Institute of Food and Agriculture. The authors would like to thank the funding agency for their continued support.

References

Agrawal, A., Chakraborty, S., 2013. A kinetic study of pyrolysis and combustion of microalgae *Chlorella vulgaris* using thermo-gravimetric analysis. Bioresour. Technol. 128, 72–80.
Blaine, R.L., Kissinger, H.E., 2012. Homer Kissinger and the Kissinger equation. Thermochim. Acta 540, 1–6.
Carrier, M., Loppinet-Serani, A., Denux, D., Lasnier, J., Ham-Pichavant, F., Cansell, F., Aymonier, C., 2011. Thermogravimetric analysis as a new method to determine the lignocellulosic composition of biomass. Biomass Bioenergy 35, 298–307.
Conley, D.J., Paerl, H.W., Howarth, R.W., Boesch, D.F., Seitzinger, S.P., Havens, K.E., Lancelot, C., Likens, G.E., 2009. Controlling eutrophication: nitrogen and phosphorus. Science 323, 1014–1015.
Damartzis, T., Vamvuka, D., Sfakiotakis, S., Zabaniotou, A., 2011. Thermal degradation studies and kinetic modeling of cardoon (*Cynara cardunculus*) pyrolysis using thermogravimetric analysis (TGA). Bioresour. Technol. 102, 6230–6238.
Demirbas, A., Fatih Demirbas, M., 2011. Importance of algae oil as a source of biodiesel. Energy Conv. Manage. 52, 163–170.
Doyle, C., 1962. Estimating isothermal life from thermogravimetric data. J. Appl. Polym. Sci. 6, 639–642.
Flynn, J.H., Wall, L.A., 1966. General treatment of the thermogravimetry of polymers. J. Res. Natl. Bur. Stand. A Phys. Chem. 70Z, 487–523.
Friedman, H.L., 1965. Kinetics of thermal degradation of char-foaming plastics from thermogravimetry: application to a phenolic resin. J. Polym. Sci. 6, 183–195.
Gai, C., Zhang, Y., Chen, W., Zhang, P., Dong, Y., 2013. Thermogravimetric and kinetic analysis of thermal decomposition characteristics of low-lipid microalgae. Bioresour. Technol. 150, 139–148.
García, R., Pizarro, C., Lavín, A.G., Bueno, J.L., 2013. Biomass proximate analysis using thermogravimetry. Bioresour. Technol. 139, 1–4.
Gomez, C.J., Varhegyi, G., Puigjaner, L., 2005. Slow pyrolysis of woody residues and an herbaceous biomass crop: a kinetic study. Ind. Eng. Chem. Res. 44, 6650–6660.
Gómez, X., Cuetos, M.J., García, A.I., Morán, A., 2007. An evaluation of stability by thermogravimetric analysis of digestate obtained from different biowastes. J. Hazard. Mater. 149, 97–105.
Heathwaite, A., 2010. Multiple stressors on water availability at global to catchment scales: understanding human impact on nutrient cycles to protect water quality and water availability in the long term. Freshwat. Biol. 55, 241–257.
Higgins, S.N., Malkin, S.Y., Todd Howell, E., Guildford, S.J., Campbell, L., Hiriart-Baer, V., Hecky, R.E., 2008. An ecological review of *Cladophora glomerata* (Chlorophyta) in the Laurentian great lakes1. J. Phycol. 44, 839–854.
Jenkins, B., Baxter, L., Miles Jr, T., Miles, T., 1998. Combustion properties of biomass. Fuel Process Technol. 54, 17–46.
Jones, D.B., 1941. Factors for Converting Percentages of Nitrogen in Foods and Feeds into Percentages of Proteins. US Department of Agriculture, Washington, DC.
Kebede-Westhead, E., Pizarro, C., Mulbry, W.W., 2006. Treatment of swine manure effluent using freshwater algae: production, nutrient recovery, and elemental composition of algal biomass at four effluent loading rates. J. Appl. Phycol. 18, 41–46.
Maddi, B., Viamajala, S., Varanasi, S., 2011. Comparative study of pyrolysis of algal biomass from natural lake blooms with lignocellulosic biomass. Bioresour. Technol. 102, 11018–11026.
Mani, T., Murugan, P., Abedi, J., Mahinpey, N., 2010. Pyrolysis of wheat straw in a thermogravimetric analyzer: effect of particle size and heating rate on devolatilization and estimation of global kinetics. Chem. Eng. Res. Des 88, 952–958.
McCoy, B.J., 1999. Distribution kinetics for temperature-programmed pyrolysis. Ind. Eng. Chem. Res. 38, 4531–4537.
Morris, M.K., 1982. Effects of Wastewater Discharges on Periphyton Growth in Lake Mead, Nevada-Arizona.
Muller-Feuga, A., 2000. The role of microalgae in aquaculture: situation and trends. J. Appl. Phycol. 12, 527–534.
Na, J., Lee, H.S., Oh, Y., Park, J., Ko, C.H., Lee, S., Yi, K.B., Chung, S.H., Jeon, S.G., 2011. Rapid estimation of triacylglycerol content of *Chlorella* sp. by thermogravimetric analysis. Biotechnol. Lett. 33, 957–960.
Ozawa, T., 1965. A new method of analyzing thermogravimetric data. Bull. Chem. Soc. Jpn. 38, 1881–1886.
Pittman, J.K., Dean, A.P., Osundeko, O., 2011. The potential of sustainable algal biofuel production using wastewater resources. Bioresour. Technol. 102, 17–25.
Sanchez, M., Otero, M., Gomez, X., Moran, A., 2009. Thermogravimetric kinetic analysis of the combustion of biowastes. Renew. Energy 34, 1622–1627.
Sharara, M., Sadaka, S., 2014. Thermogravimetric analysis of swine manure solids obtained from farrowing, and growing-finishing farms. J. Sust. Bioenergy Syst. 4, 75–86.
Skulberg, O.M., 2004. 30 Bioactive chemicals in microalgae. Handbook of Microalgal Culture: Biotechnology and Applied Phycology, p. 485.
Starink, M., 2003. The determination of activation energy from linear heating rate experiments: a comparison of the accuracy of isoconversion methods. Thermochim. Acta 404, 163–176.
Teng, H., Wei, Y., 1998. Thermogravimetric studies on the kinetics of rice hull pyrolysis and the influence of water treatment. Ind. Eng. Chem. Res. 37, 3806–3811.
Vyazovkin, S., 1996. A unified approach to kinetic processing of nonisothermal data. Int. J. Chem. Kinet. 28, 95–101.
Xin, L., Hong-ying, H., Ke, G., Ying-xue, S., 2010. Effects of different nitrogen and phosphorus concentrations on the growth, nutrient uptake, and lipid accumulation of a freshwater microalga *Scenedesmus* sp.. Bioresour. Technol. 101, 5494–5500.
Yao, F., Wu, Q., Lei, Y., Guo, W., Xu, Y., 2008. Thermal decomposition kinetics of natural fibers: activation energy with dynamic thermogravimetric analysis. Polym. Degrad. Stab. 93, 90–98.
Zhao, H., Yan, H., Dong, S., Zhang, Y., Sun, B., Zhang, C., Ai, Y., Chen, B., Liu, Q., Sui, T., 2013. Thermogravimetry study of the pyrolytic characteristics and kinetics of macro-algae *Macrocystis pyrifera* residue. J. Therm. Anal. Calorim. 111, 1685–1690.